https://doi.org/10.30799/jnst.sp203.18040203 J. Nanosci. Tech. - Volume 4 Issue 2 (2018) 348–352

Share Your Innovations through JACS Directory

Journal of Nanoscience and Technology

Visit Journal at http://www.jacsdirectory.com/jnst

ISSN: 2455-0191

Special Issue on "International Conference on Nanomaterials - 2018" – Alagappa University *Issue Editor:* Dr. G. Ramalingam

Spectra, Electronic Properties, Biological Activities and Molecular Docking Investigation on Sulfonamide Derivative Compound: An Experimental and Computational Approach

V. Vetrivelan*

Department of Physics, Thanthai Periyar Government Institute of Technology, Vellore – 632 002, Tamilnadu, India.

ARTICLE DETAILS

Article history:
Received 21 March 2018
Accepted 28 March 2018
Available online 06 April 2018

Keywords:
DFT Calculation
NBO
Molecular Docking

ABSTRACT

The title compound methyl (2E)-2-{[N-(2-formylphenyl)-4-methylbenzene sulfonamido] methyl}-3-phenylprop-2-enoate (MFMSPE) is a derivative of sulfonamide. FT-IR spectra of MFMSPE in the solid phase were recorded and analyzed. The optimized geometry and vibrational wave numbers were computed using DFT/B3LYP method with aid of 6-311++G (d,p) basis set. Stability of the molecule arising from hyper conjugative interactions, charge delocalization has been analyzed using natural bond orbital (NBO) analysis. The calculated HOMO and LUMO energies confirm that charge transfer occurs within the molecule. Molecular electrostatic potentials (MEP) was carried out at and interpreted. To recognize the biological activity of MFMSPE, molecular docking was done to recognize the hydrogen bond lengths and binding energy with antibacterial protein (1KE4).

1. Introduction

Sulfonamides are the primary economical chemotherapeutic agents used for several years to heal or avoid general microorganism infections. It plays an important role as key constituent in range of biologically active molecules. Sulfonamides are showing associate degree ample form of biological activities such as antibacterial [1], antifungal [2], anti-inflamatory [3], anti HIV [4] and antitubercular activities [5]. Because of wide-ranging multiplicity of biological importance of the sulfonamides, synthesis of several substituted sulfonamides, their crystal structure, physical, chemical and biochemical studies has become interesting field in research. The MFMSPE compound is one alike organic compound that follows to the sulfa drug family. Literature survey reveals that to the best of my knowledge, there is no DFT, vibrational assignments, MEP, HOMO-LUMO, antimicrobial and molecular docking studies for the title compound MFMSPE. Considering these biological importance of MFMSPE, this work is primarily focused to the complete structural behavior of the molecule. FT-IR spectra of MFMSPE have been reported together with the vibrational assignments supported by PED. HOMO-LUMO study has been performed which aid to clarify charge transfer occurring in the molecule. Docking investigation has been executed to find out the hydrogen bond lengths, binding energy and drug activity of title compound.

2. Experimental Methods

2.1 Characterization

All of the chemical reagents and solvents were purchased from commercially available suppliers and used without further purification. FT-IR spectrum was obtained in the region 4000-400 cm^{-1} using Shimadzu FT-IR 8400 spectrophotometer. The anti-microbial activity of MFMSPE was screened against gram negative & positive bacterial strains and fungal strains. All the antimicrobial studies were done by using Kirby-Bauer disc diffusion method as per CLSI M38-A guidelines. The standard antibiotic such as ciprofloxacin (25 µg) and amphotericin-B (20 µg) was used as a positive control to execute the antibacterial and antifungal activity. The solution of MFMSPE in DMSO at various concentrations of 25, 50 and 75 µg/mL were examined against the bacterial and fungal strains.

2.2 Computational Details

Entire theoretical calculations of MFMSPE were work out by DFT/B3LYP method with 6-311++G (d,p) basis set using Gaussian 09 software package [6]. Gauss view molecular visualization program [7] is used to visualize the geometry structure. The theoretical vibrational assignments were interpreted by means of PED (Potential Energy Distribution) using VEDA 4 program [8]. Molecular docking studies give vital details about orientation of MFMSPE (ligand) which regulate the binding affinity between the ligand and their protein target. Molecular docking studies were carried out using Auto Dock 4.2 software [9].

3. Results and Discussion

3.1 Molecular Geometry

The numbering system adopted within the molecular structure of MFMSPE is obtained from Gaussian 09W and GaussView 5.0 programs are shown in Fig. 1. The bond parameters (bond length, bond angles and torsional angles) of the MFMSPE molecules are listed in Table 1 using DFT/B3LYP method with 6-311++G (d,p) basis set. From the computed values, it is found that almost all of the optimized molecular bond lengths are slightly beyond the experimental values because of the very fact that the theoretical calculations were applied isolated molecule in the gas phase and the experimental XRD results were applied within the solid state.

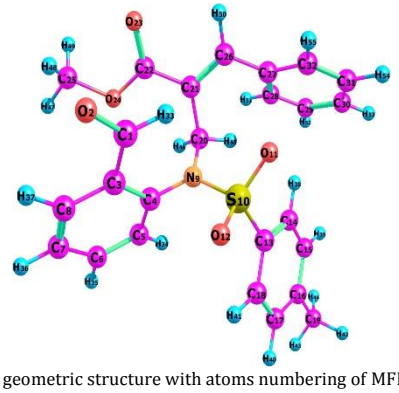

Fig. 1 Optimized geometric structure with atoms numbering of MFMSPE

*Corresponding Author: vetri.tpgit@gmail.com(V. Vetrivelan)

https://doi.org/10.30799/jnst.sp203.18040203

Cite this Article as: V. Vetrivelan, Spectra, electronic properties, biological activities and molecular docking investigation on sulfonamide derivative compound: an experimental and computational approach, J. Nanosci. Tech. 4(2) (2018) 348–352.

Table 1 Selected geometry parameters by XRD and DFT calculations of MFMSPE

Atoms	XRD [10]	DFT	Atoms	XRD [10]	DFT	Atoms	XRD [10]	DFT
Bond lengths			Bond angles			Torsional angles		
C4-N9	1.438(2)	1.445	C3-C7-N9	118.9(2)	120.6	N9-C4-C3-C8	178.9(2)	178.7
C3-C1	1.395(2)	1.397	O2-C1-C3	124.2(2)	123.7	N9-C4-C3-C1	3.9(2)	3.2
C1-O2	1.197(2)	1.203	C18-C13-S10	119.9(1)	118.8	C14-C15-C16-C19	-177.7(2)	-178.2
C13-S10	1.758(2)	1.782	C14-C13-S10	120.0(1)	119.7	C19-C16-C17-C18	177.3(2)	177.7
C20-N9	1.488(2)	1.495	O23-C22-O24	122.7(2)	123.6	C21-C20-N9-S10	-87.0 (1)	-87.6
C22-O23	1.201(2)	1.205	O23-C22-C21	123.7(2)	122.9	O23-C22-O24-C25	-0.1(3)	-0.7
C22-O24	1.330(2)	1.337	O24-C22-C21	113.6(2)	112.5	C21-C22-O24-C25	178.9(2)	179.7
C25-O24	1.441(2)	1.433	C4-N9-C20	118.1(1)	118.7	C9-C13-S10-N9	-81.2(2)	-78.5
N9-S10	1.649(1)	1.671	C4-N9-S10	117.1(1)	117.9	C18-C13-S10-N9	-92.4(2)	-95.6
O12-S10	1.428(1)	1.438	C20-N9-S10	116.3(1)	116.9			
O11-S10	1.427(1)	1.442	C22-O24-C25	116.9(2)	115.7			
			O11-S10-O12	119.6(1)	120.5			
			O11-S10-N9	106.3(1)	105.4			
			O12-S10-N9	106.6(4)	106.9			
			O11-S10-C13	108.2(4)	107.7			
			O12-S10-C13	107.9(1)	108.5			
			N9-S10-C13	108.4(1)	107.7			

Table 2 Observed and calculated frequencies of MFMSPE

Experimental wavenumbers (cm^{-1})	Calculated wavenumbers (cm^{-1})		Vibrational assignments PED(%)[b]
	Unscaled	Scaled*	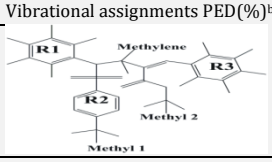
3047	3182	3058	νCH(97) in Ring3
2989	3091	2970	υ_{as}CH(19) in Methyl 1 + υ_{as}CH(80) in Methyl 1
2893	3063	2944	νCH(99) in C1-H34
2775	3047	2928	υ_{s}CH(85) in $C19H_3$(Methyl 1)+ υ_{s}CH(15) in $C19H_3$(Methyl 1)
1743	1792	1722	υ_{s}OC(92) in O23-C22
	1785	1715	νOC(93) in O2-C1
1565	1658	1593	νCC(54) +β HCC(20) in Ring 2
1469	1548	1488	asymd HCH(15) in $C25H_3$ (Methyl 2) +τ HCOC(18) + γHCH(69) in $C25H_3$(Methyl 2)
	1434	1378	ω HCH(93) in $C19H_3$(Methyl 1)
1343	1392	1338	β HCH(27) in H51-C26-C27 + τHCCC(39) in H47-C20-C21-C26+ ω HCH(15) in CH_2
1291	1346	1294	β HCC(15) in Ring3+ νSO(49)in S10-O12
	1257	1208	νCC(18) in Ring 3+ νNC(17) N9-C4+ νCC(25) in C17-C18
	1249	1200	νCC(31) in C19-C16+ νNC(19) N9-C4
	1242	1194	r HCH(41) in $C25H_3$ (Methyl 2) +τHCOC(61)in CO_2CH_3
1083	1198	1151	τHCOC(67) in CO_2CH_3+ rHCH(26)in $C25H_3$ (Methyl 2)
	1161	1116	νSO(81)in S10-O11
1064	1063	1022	β HCC(17) in Ring 3+ νCC(63) in Ring 3
758	754	725	νSN(18)in S10-N9
	669	643	outONOS(10) inO11-N9-O12-S10+ β CCC(17) in Ring 1
675	670	644	νSC(18)+ β CCC(26) in Ring 1+ outONOS(18) inO12-N9-O12-S10
589	653	628	β CCN(17) in C5-C4-N9+ outOCOC(23) in O23-C21-O24-C22
548	588	565	outONOS(19) inO11-N9-O12-S10+ ρOSO(30) inO11-S10-O12
	548	527	ω OSO(18) in SO_2+ τCCCC(31) in Ring 3
	537	516	β CCN(32) in C5-C4-N9+ τCCCC(19) in Ring 3
482	501	481	γOCC(21) in O24-C22- C21+ τCCCC(35) in Ring 1
	357	343	γCOC(64) in C22-O24- C25
	339	326	γCNC(26) in C4-N9- C20
	319	307	γOSC(24) in O12-S10-C13
	284	273	νSC(24) in S10-C13 +outONOS(19) inO11-N9-O12-S10
	274	263	νSC(29) in S10-C13+ γCCC(21) in Ring 2
	231	222	γCNS(14) in C20-N9- S10+ outClCCC(25) in Ring 3
	149	143	γCCN(18) in C21-C20-N9
	131	126	γCNS(19) in C20-N9- S10
	53	51	γNSC(26) in N9-S10-C13+outSCCC(31) in S10-C14-C18–C3

*ν-stretching; ν_s-symmetric stretching; ν_{as}- asymmetric stretching; β- in plane bending; γ-out of plane bending; ω-wagging; t-twisting; ρ- scissoring; r-rocking; τ-torsion; symd-symmetric deformation; asymd-asymmetric deformation; *Scaling factor:0.961 for DFT/(B3LYP/6-311G(d,p)); [b] PED less than 10% are not shown*

Table 3 Second order perturbation theory analysis of fock matrix in NBO basis for MFMSPE

Donor(i)	Type	E_D(i)(e)	Acceptor(j)	Type	E_D(j)(e)	E(2)[a] (kJmol^{-1})	E(i)-E(j)[b] (a.u.)	F(i,j)[c] (a.u.)
O11	LP(3)	1.89435	S10-O12	σ*	0.24734	19.71	0.65	0.171
			S10-N9	σ*	0.37276	18.20	0.56	0.098
O13	LP (2)	1.84245	O24 – C25	π*	0.31647	46.53	0.38	0.121
O23	LP (2)	1.83621	S10 – C20	σ*	0.18671	17.48	0.42	0.081
O23	LP (3)	1.80923	S10 – O13	σ*	0.12354	18.36	0.61	0.088
	LP (3)	1.79919	S10 – N9	σ*	0.25917	16.28	0.44	0.074
O24	LP (2)	1.86443	C21 – C22	σ*	0.08655	32.69	0.68	0.131
	LP (2)	1.86422	C32 - C31	σ*	0.05452	17.82	0.71	0.091

E_D means electron density; [a]E(2) means energy of hyper conjugative interactions; [b]Energy difference between donor and acceptor i and j NBO orbitals; [c]F(i,j) is the Fock matrix element between i and j NBO orbitals

https://doi.org/10.30799/jnst.sp203.18040203

Cite this Article as: V. Vetrivelan, Spectra, electronic properties, biological activities and molecular docking investigation on sulfonamide derivative compound: an experimental and computational approach, J. Nanosci. Tech. 4(2) (2018) 348–352.

3.2 Vibrational Analysis

Vibrational spectroscopy is employed extensively in organic chemistry for the identification of functional groups of organic compounds, the study of molecular confirmations, kinetics, reaction etc. The title molecule consists of 55 atoms, which has 159 normal modes of vibration. PED was computed for every normal mode among the symmetry coordinates of the molecule. Based on the computed PED values and FT-IR intensities activities a detailed assignment of the fundamentals was suggested. All the theoretical vibrational assignments of MFMSPE were computed using VEDA 4 program and interpreted with PED analysis**.** The vibrational wavenumbers were computed by DFT/B3LYP method with 6-311++G (d, p) basis set. The selected experimentally observed and theoretically calculated vibrational wavenumbers were compared and reflected in Table 2. The computed vibrational wavenumbers atB3LYP/6-311G++(d,p) level were scaled by 0.961 so as to correct the theoretical error during this work. The comparison of experimental and theoretical FT-IR spectra is shown in Fig. 2.

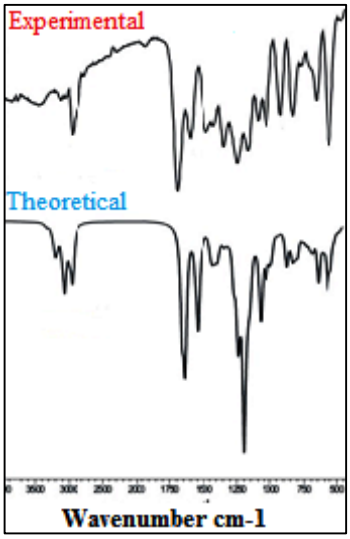

Fig. 2 Experimental and theoretical FT-IR spectra of MFMSPE

The C-H stretching vibrations of ring are within the region 3080-3010 cm^{-1} that is that the characteristic region for the identification of C-H stretching vibration [11]. The bands are not affected during region because of the character of substituents. The C-H stretching vibrations of MFMSPE are computed within the range of 3058- 2944 cm^{-1} in FT-IR spectrum.

C-H stretching spectral position of methyl radical and methylene radical teams is at lower frequencies than those of aromatic C-H ring stretching.CH_3 and CH_2 asymmetric and symmetric stretching vibrations are typically ascertained within the region 3100-2900 cm^{-1} and 2900-2800 cm^{-1} respectively [12]. CH_3 asymmetric and symmetric stretching vibrations are ascertained at 2989 and 2775 cm^{-1} in IR, respectively, with major PED contribution of 99% as shown in Table 2. CH_3 asymmetric and symmetric bending vibrations unremarkably seem within region 1470-1440 cm^{-1} and 1390-1370 cm^{-1} respectively. Asymmetric bending vibration is ascertained at 1469 in IR as a medium band whereas symmetric bending vibration is ascertained at 1343 in IR as a medium band. The observed values are in good agreement with the scaled values as listed in Table 2.

C=O stretching band seems powerfully within the region 1870-1540 cm^{-1} within which the position of C=O stretching band depends on the physical state, electronic and mass effects of the neighboring substituents, conjugations, intra and intermolecular hydrogen bonding. In MFMSPE, the terribly strong absorptions at 1743 cm^{-1} in IR is allotted to C=O stretching modes. From the above results, it is found that the intensities of these bands are terribly high and also the computed values of the force constants are terribly large. Such intense IR absorption bands are ascertained because of the very fact that, the multiple bonded carbonyl groups is highly polar. Obviously, these modes are pure stretching modes that are evident from the PED column and the PED values support the experimental values. In-plane and out-of-plane bending vibrations have conjointly been known and listed in Table 2.

The symmetric and asymmetric SO_2 stretching vibrations belong to the region 1150-1125cm^{-1} and 1330-1295 cm^{-1}, respectively [13]. In MFMSPE, a band in FT-IR spectrum at 1291 cm^{-1} is selected to SO_2 stretching mode and computed wave number at 1294cm^{-1} with PED contribution of 49%. The region of the SO_2 scissoring (560±40 cm^{-1}) which of SO_2 wagging vibration (500±55 cm^{-1}) partially overlap; the two vibrations show distinctly [14]. In the present study, FT-IR band ascertained at 548 cm^{-1} is allotted to SO_2 scissoring. The theoretically calculated values at 565 and 527 cm^{-1} are selected to SO_2 scissoring and wagging vibrations, respectively.

3.3 Donor-Acceptor Interactions (NBO Analysis)

Natural Bond Orbital (NBO) analysis utilizes an additional refined scheme that uses the thought of natural orbitals and occupation-based symmetric orthogonalization that results in additional strong results. The NBO analysis has been performed for MFMSPE using DFT/B3LYP/6-311++G (d, p) level, that explains the second-order interactions between filled-orbital of one sub-system and vacant orbital of another sub-system. The NBO analysis assesses intermolecular delocalization or hyper conjugation of the system. The second-order Fock matrix [15] was introduced for the donor-acceptor interactions. The second order perturbation theory analysis of Fock-matrix in NBO basis for MFMSPE is shown in Table 3. This technique is additionally wont to analyze the interaction between each filled and virtual orbital areas that strengthen the analysis of intra molecular interactions. Due to these intense interactions, there is loss of occupancy from localized Lewis orbital to an empty non-Lewis orbital. The NBO analysis provides the electronic density distribution on atoms and bonds. It is clear from Table 3 that the solid intermolecular hyper conjugative interaction of the π and σ electrons of C-C to the anti-bond C-C of the ring is accountable for the stabilization of certain part of the ring.

3.4 HOMO-LUMO Analysis

There are 2 sets of energy levels for α and β electrons having opposite spins that correspond to cations and anions. Theα molecular orbitals are HOMO (highest occupied molecular orbitals) and β molecular orbitals are LUMO (Lowest unoccupied molecular orbitals). These Frontier molecular orbitals (HOMO and LUMO) have vital role to check concerning optical, electrical properties, quantum chemistry and UV-Vis spectra [16]. The stability of the compound, chemical and spectroscopic studies is represented by the HOMO - LUMO energy gap.

In view of this, the frontier electron density describes numerous sorts of reactions in coupled systems and additionally computing the foremost necessary reactive sites in π-electron systems. The energy gap is that the outcome of intra molecular charge transfer from electron donor groups to the acceptor groups through π-conjugated orbit. Higher E_{HOMO} value indicates that the molecules have a lot of tendencies to donate electrons. On the other hand, lower the value of E_{LUMO} suggests that molecules have a lot of tendencies to simply accept electrons. The FMO energy values are used to compute the electronic band gaps and therefore the chemical reactions of the compound MFMSPE. The HOMO and LUMO plot and its energy gap is shown in Fig. 3. The computed HOMO and LUMO values for MFMSPE are -6.6956 eV and -2.2049 eV and therefore the energy gap was calculated as 4.4907 eV respectively. The lower energy gap value of MFMSPE describes the intra molecular charge that induces chemical and biological activities.

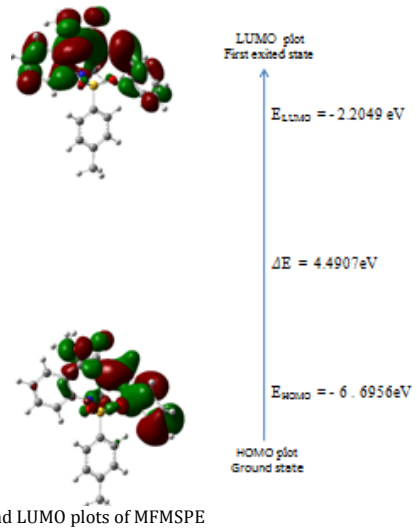

Fig. 3 HOMO and LUMO plots of MFMSPE

3.5 Global and Local Reactivity Descriptors

The chemical reactivity descriptors [chemical potential (μ), chemical hardness (η), electronegativity (χ) and electrophilicity index (ω)] of

https://doi.org/10.30799/jnst.sp203.18040203

MFMSPE were computed using DFT method with B3LYP/6-311++G (d,p) basis set and the corresponding values are recorded in the Table 4. These descriptors have been computed using HOMO and LUMO energy values of MFMSPE.

Table 4 Calculated energy values of MFMSPE

Basis set	B3LYP/6-311++G(d,p)
HOMO(eV)	-6.6956
LUMO(eV)	-2.2049
Ionization potential	6.6956
Electron affinity	2.2049
Energy gap(eV)	4.4907
Electronegativity	4.4503
Chemical potential	-4.4503
Chemical hardness	2.2454
Chemical softness	0.2227
Electrophilicity index	4.4102

3.6 Molecular Electrostatic Potential (MEP)

MEP analysis describes the electrophilic attack, nucleophilic reaction and hydrogen bonding interactions of the molecule. The shape, size, charge, density and reactive sites of the molecule are described by an electron density isosurface mapped with electro potential surface. MEPs map and contour plot of MFMSPE created at optimized geometry of compound using Gauss view 5.0 program is shown in Figs. 4 and 5. The Fig. 4 shows that the scrutinized molecule has several possible sites of electrophilic and nucleophilic attack. The deepest blue indicating extremely electron deficient region and deepest red indicating electron rich region are shown in Fig. 4. The obtained MEP map shows that the positive potential sites are around hydrogen (H) atoms and the negative potential sites are on oxygen (O) and nitrogen (N) atoms. These active sites found to be clear evidence of biological activity in MFMSPE.

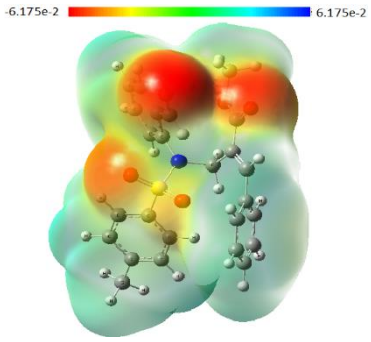

Fig. 4 MEP on MFMSPE

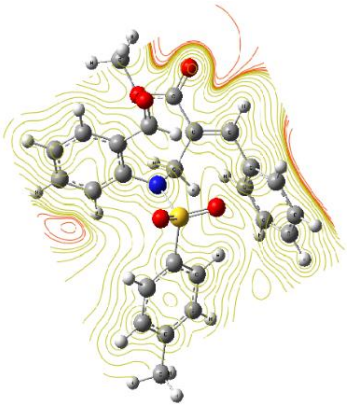

Fig. 5 Contour map on MFMSPE

3.7 Interpretation of Antimicrobial Activity

The anti-microbial activity of MFMSPE was tested using *in-vitro* disc diffusion method against gram negative & positive bacterial strains and fungal strains. The standard antibiotic such as Ciprofloxacin (25 µg) and amphotericin-B (20 µg) was used as a positive control to perform the antibacterial and antifungal activity.

The target compound MFMSPE showed antimicrobial activity at different concentrations against bacterial and fungal pathogens and are shown in Table 5. As a result, the compound MFMSPE detected as an essential antibacterial drug. The results obtained from the antimicrobial activity of MFMSPE verified the molecular docking result.

Table 5 In vitro antibacterial and antifungal activity of MFMSPE at different concentrations against selected pathogens.

Micro organisms	Zone of inhibition(mm)			
	Compound concentration			Positive control
	25 µg/mL	50 µg/mL	75 µg/mL	
Bacterial Pathogens				
Gram Positive				Ciprofloxacin 25 µg/mL
Staphylococcus aureus	22	26	32	28
Staphylococcus epidermidis	17	24	28	22
Gram Negative				
Escherichia coli	21	27	33	26
Acinetobacter baumanni	15	22	28	25
Fungal Pathogens				Amphotericin-B 20 µg/mL
Candida albicans	19	26	35	25
Aspergillus niger	13	19	25	22
Monascus purpureus	12	19	26	23

**Values are mean of three independent experiments*

3.8 Molecular Docking

Molecular docking was performed against 1KE4 and its purpose is to estimate the binding modalities of MFMSPE. Hydrogen bonding plays an important role in the structure and function of biological molecules, the ligand-receptor interactions were inspected on the basis of hydrogen bonding. Table 6 showed the corresponding binding energy, interactions, distance and the bonding type. It is evident from Table 6, the synthesized ligand molecule MFMSPE is tightly fitted with the active position of 1KE4 with very good binding energy -4.64 kcal/mol as shown in Fig. 6.

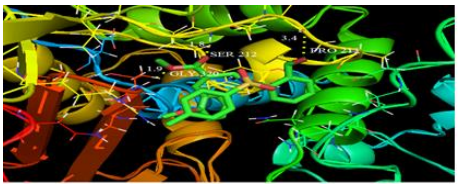

Fig. 6 Docking and hydrogen bond interaction of MFMSPE with 1KE4

Table 6 Molecular docking with 1KE4

Protein (PDB ID)	Bonded residues	No. of hydrogen bond	Bond distance (Å)	Estimated Inhibition Constant (µm)	Binding energy (kcal/mol)	Reference RMSD (Å)
1KE4	GLY-320 SER-212 PRO-213	3	1.9 1.8 3.4	395.62	-4.64	58.2

4. Conclusion

Methyl (2E)-2-{[N-(2-formylphenyl)-4-methylbenzene sulfonamido] methyl}-3- phenylprop-2-enoate (MFMSPE) was characterized by FTIR. The geometric parameters, vibrational frequencies MFMSPE have been computed using DFT/B3LYP method with 6-311++G(d,p) as basis set and are in good agreement with the experimental results. NBO analysis result shows that electron density(E_D) in the π* and σ* antibonding orbitals and second order delocalization energies $E_{(2)}$ prove the occurrence of intra molecular charge transfer (ICT) within the molecule and causing stability of the molecule. The lowering of the HOMO-LUMO energy gap value has extensive influence on the intra molecular charge transfer and bioactivity of the molecules. Molecular docking of the title compound is also reported due to the different biological activity of MFMSPE. Therefore, we hope the results of this present study will facilitate researchers to explore and synthesize of new compounds.

References

[1] N. Subhakara Reddy, Srinivas Rao, M. Adervana Chari, V. Ravikumara, V. Jyothyc, V. Himabindu, Synthesis and antibacterial activity of sulfonamide derivatives at C-8 alkyl chain of an acardic acid mixture isolated from a natural product cashew nut shell liquid (CNSL), J. Chem. Sci. 124(3) (2012) 723-730.

[2] A. Hanafy, J. Uno, H. Mitani, Y. Kang, Y. Mikami, In vitro antifungal activities of sulfa drugs against clinical isolates of Aspergillus and Cryptococcus species, Jpn. J. Med. Mycol. 48(1) (2007) 47-50.

[3] S. Guniz Kucukguzel, Inci Coskun, Azize Sener, Neerja Kausik Basu, Amartya Basu, T.T. Talele, Synthesis and characterization of celecoxib derivatives as

https://doi.org/10.30799/jnst.sp203.18040203

Cite this Article as: V. Vetrivelan, Spectra, electronic properties, biological activities and molecular docking investigation on sulfonamide derivative compound: an experimental and computational approach, J. Nanosci. Tech. 4(2) (2018) 348–352.

possible anti-inflammatory, analgesic, antioxidant, anticancer and anti-HCV agents, Molecules 18 (2013) 3595-3614.
[4] J.D. Warren, D.L. Woodward, R.T. Hargreaves, 4-Substituted semicarbazones of mono- and dichlorobenzaldehydes as antihypertensive agents, J. Med. Chem. 20(11) (1977) 1520-1521.
[5] C.T. Supuran, A. Scozzafava, Carbonic anhydrase inhibitors: aromatic sulfonamides and disulfonamides act as efficient tumor growth inhibitors, J. Enzyme Inhib. Med. Chem. 15 (2000) 597-610.
[6] M.J. Frisch, Gaussian 09, Gaussian Inc., Wallingford, CT, USA, 2009.
[7] R. Dennington, T. Keith, J. Millam, Gauss View, Version 4.1.2, Semichem Inc. Shawnee Mission, KS, 2007.
[8] M.H. Jamroz, Vibrational energy distribution analysis VEDA 4, Warsaw, 2004-2010.
[9] O. Trott, A.J. Olson, AutoDock Vina: Improving the speed and accuracy of docking with a new scoring function, efficient optimization, and multithreading, J. Comput. Chem. 31 (2010) 455-461.
[10] R. Madhanraj, S. Murugavel, D. Kannan, M. Bakthadoss, Methyl(Z)-2-{[N-(2-formylphenyl)-4-methylbenzenesulfonamido]methyl}-3-phenylprop-2-enoate, Acta Cryst. E 67(12) (2011) 3511.
[11] V.K. Rastogi, M.A. Palafox, R.P. Tanwar, L. Mittal, 3,5-Difluorobenzonitrile: ab initio calculations, FTIR and Raman spectra, Spectrochim. Acta A 58 (2002) 1987-2004.
[12] B. Smith, Infrared spectral interpretation – A schematic approach, CRC Press, New York, 1999.
[13] G. Socrates, Infrared and Raman characteristic group frequencies: Tables and charts, Wiley, John & Sons, Chichester, New York, 2001.
[14] L.J. Bellamy, The infrared spectra of complex molecules, Vol. 2, Chapman and Hall, London, 1980.
[15] M. Szafran, A. Komasa, E.B. Admska, Crystal and molecular structure of 4-Carboxy piperidinium chloride (4-piperidinecarboxylic acid hydrochloride), J. Mol. Struct. Theochem. 827 (2007) 101-107.
[16] I. Fleming, Frontier orbitals, organic chemical reactions, Wiley, London, 1976.

***About the Conference*:** "International Conference on Nanomaterials (ICAN) - 2018" has been organized by Dr. G. Ramalingam, ICAN-2018 Organizing Secretary, Assistant Professor, Department of Nanoscience and Technology, Alagappa University, Karaikudi, TN, India at his designated venue on 26th & 27th February 2018.

https://doi.org/10.30799/jnst.sp203.18040203

Cite this Article as: V. Vetrivelan, Spectra, electronic properties, biological activities and molecular docking investigation on sulfonamide derivative compound: an experimental and computational approach, J. Nanosci. Tech. 4(2) (2018) 348–352.